Journal of Power Sources 195 (2010) 380–383

Contents lists available at ScienceDirect

Journal of Power Sources

journal homepage: www.elsevier.com/locate/jpowsour

Short communication

Effect of CuO addition on electrochemical properties of AB_3-type alloy electrodes for nickel/metal hydride batteries

Yuan Li [a], Shumin Han [a,b,*], Xilin Zhu [a], Huiling Ding [a]

[a] Department of Environmental and Chemical Engineering, Yanshan University, Qinhuangdao 066004, PR China
[b] State Key Laboratory of Metastable Materials Science and Technology, Yanshan University, Qinhuangdao 066004, PR China

ARTICLE INFO

Article history:
Received 25 December 2008
Received in revised form 16 June 2009
Accepted 30 June 2009
Available online 7 July 2009

Keywords:
Ni/MH batteries
Hydrogen storage alloys
CuO
Additives
Electrochemical properties

ABSTRACT

In order to improve overall electrochemical properties of AB_3-type hydrogen storage alloy electrodes, especially the cycling stability, CuO was added to the electrode. Electrochemical properties of the electrodes with and without additives were studied. Cyclic voltammetry and SEM results show that CuO is reduced to Cu during the charging process and the fine Cu particles deposit at surface of the alloy particles. The as-deposited Cu particles form a protective layer to increase electronic and heat conductivity of the electrodes and thus improve maximum discharge capacity, high rate dischargeability, cycling stability and dischargeability at high temperature of the electrodes. The maximum discharge capacity increases from 314 mAh g^{-1} (blank electrode) to 341 mAh g^{-1} (3.0 wt.% CuO) and the capacity retention rate at the 200th cycle increases from 71.6% to 77.2% (2.5 wt.% CuO).

© 2009 Elsevier B.V. All rights reserved.

1. Introduction

Nickel/metal hydride (Ni/MH) batteries have been widely used in portable electronic devices, electric hand tools and even hybrid electric vehicles (HEV) because of their good performance and environmental friendliness [1]. However, the discharge capacity of commercial AB_5-type rare earth-based alloys cannot be greatly improved, which is unfavorable to further development of Ni/MH batteries [2,3]. Some recent research show that La–Mg–Ni-based AB_3-type alloys will be potential negative electrode materials of Ni/MH batteries for their comparatively higher discharge capacity, but this type of alloys are subject to poor cycling stability [4–8].

Recent research found that additives, including carbon-based materials, fluoride, metal oxide, etc, could greatly improve charge/discharge characteristics of Ni/MH batteries. The carbon nanotubes were considered as effective additives to Ni/MH batteries, to the negative electrodes or to the positive electrodes. Wu et al. and Zhang et al. found the capacity and cycling stability of the batteries were enhanced and the inner resistance was reduced when discharging at high current density by adding carbon nanotubes to the positive and negative electrodes, respectively [9,10]. The use of $Co(OH)_2$-coated $Ni(OH)_2$ plus a CaF_2-addition to the positive electrode was believed to increase high temperature dischargeability of Ni/MH batteries [11]. It is claimed that transition metals (TMs) combined with oxygen play an important role during the sorption process, which was probably related to the improved electronic exchange reactions with hydrogen molecules [12,13]. Metal oxides, such as CuO, CoO, TiO_2 and ZnO added to the MH electrode or the electrolyte can form a protective layer to prevent oxide of lanthanide, and therefore improve service life of the electrodes [14–17]. Nb_2O_5 was believed to improve hydrogen sorption kinetics of magnesium due to its catalytic effect [18]. However, the exact mechanism of transition metal oxide on electrode reactions was not clear. The heavy rare earth oxide was favorable to properties of Ni/MH batteries either as an additive to the $Ni(OH)_2$ electrode, or as an additive to the MH electrode. When they were added to $Ni(OH)_2$ electrode, oxygen evolution was suppressed in the final charging stage, which in turn restrains corrosion of MH electrodes by oxygen; on the other hand, they were added to rare earth based AB_5-type MH electrode, dissolution of lanthanide from the hydrogen storage alloy was inhibited [19].

Metal oxide additives were believed to improve electrochemical properties of AB_5-type alloys, Mg-based alloys and so on. But as for the La–Mg–Ni-based AB_3-type hydrogen storage alloys, effect of additives on this type of alloy electrodes was less reported. In order to improve electrochemical properties of AB_3-type alloys, CuO was added to the electrode, and its effect on microstructure and electrochemical properties is studied in this paper.

* Corresponding author at: Department of Environmental and Chemical Engineering, Yanshan University, Qinhuangdao 066004, PR China. Tel.: +86 335 8074648; fax: +86 335 8074648.
E-mail address: hanshm@ysu.edu.cn (S. Han).

0378-7753/$ – see front matter © 2009 Elsevier B.V. All rights reserved.
doi:10.1016/j.jpowsour.2009.06.093

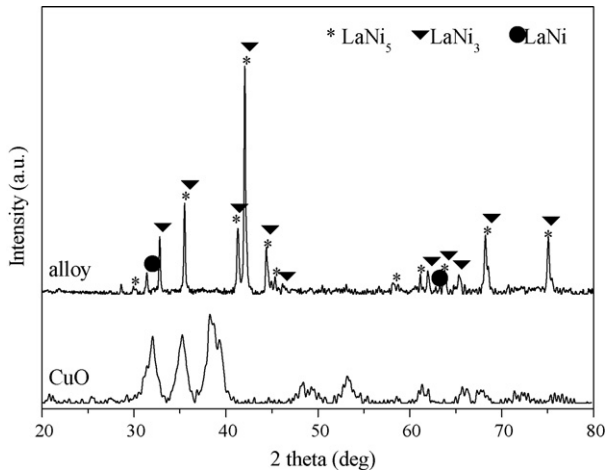

Fig. 1. XRD pattern of $La_{0.88}Mg_{0.12}Ni_{2.95}Mn_{0.10}Co_{0.55}Al_{0.10}$ alloy and as-prepared CuO.

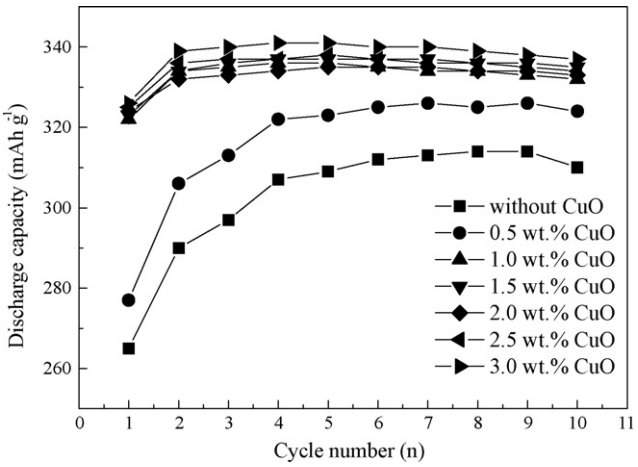

Fig. 2. Activation curves of electrodes with and without CuO additive.

2. Experimental

$La_{0.88}Mg_{0.12}Ni_{2.95}Mn_{0.10}Co_{0.55}Al_{0.10}$ alloy was prepared by inductive melting La, Mg, Ni, Co, Mn and Al (purity ≥ 99.5%) under argon atmosphere, followed by annealing at 1173 K for 8 h. The chemical composition was finally examined by ICP analysis. Then the ingots were mechanically pulverized in the air. Powders of 200–400 meshes were used for electrochemical test and powders below 300 meshes for XRD examination.

The CuO compound was synthesized by solid-state reaction. 2.00 g NaOH and 4.28 g $CuCl_2{\cdot}2H_2O$ was separately milled in the mortar for 10 min and then they were mixed and the mixture was milled for another 30 min until they turn completely black. Then the paste was washed with diluted water and ethanol for several times. The precipitation was finally dried under vacuum at 323 K.

0.34 g alloy powders, CuO additives (0.5 wt.%, 1.0 wt.%, 1.5 wt.%, 2.0 wt.%, 2.5 wt.% and 3.0 wt.% of the alloys) and 0.06 g carbonyl nickel powders were mixed with two drops of 3 wt.% poly vinyl alcohol (PVA) solution. The slurry was pasted onto both side of a foamed nickel (1.8 cm × 1.8 cm), dried completely in vacuum at 333 K, and finally cold pressed under 10 MPa. Electrochemical tests were performed in a half-cell consisting of metal hydride as working electrode, $Ni(OH)_2$/NiOOH as counter electrode and 6 mol L^{-1} KOH solution as electrolyte on DC-5 battery testing instrument at 298 K. The electrodes were fully charged (over-charged ratio was approximately 50%) at current density of 72 mA g^{-1}, and then discharged at the same current density to cut-off voltage of 1.0 V during charge/discharge test. Discharge capacities were measured at different discharge current densities when high rate dischargeabilty (HRD) was measured. The interval between charge and discharge is 10 min.

X-ray diffraction (XRD) patterns were obtained on a D/Max-2500/PC X-ray diffractometer (Cu Kα radiation). Phase identification was carried out using Jade-5.0 software. Morphology of the alloys was observed by KYKY-2800 scanning electron microscopy and KEVEX-SIGMA LEVEL4 energy dispersive spectrometry. Cyclic voltammograms were obtained on a ZF-9 potentiostat by scanning electrode potential at the rate of 50 mV min^{-1} from −1200 mV to 400 mV (vs. Hg/HgO reference electrode).

3. Results and discussion

Fig. 1 shows XRD pattern of the as-prepared $La_{0.88}Mg_{0.12}Ni_{2.95}Mn_{0.10}Co_{0.55}Al_{0.10}$ alloy and CuO compound. It can be seen that the alloy consists of $CaCu_5$-type $LaNi_5$ phase, $PuNi_3$-type $LaNi_3$ phase and some minor LaNi impurity. As for the patterns of CuO compound, XRD analysis shows that it is identical with the CuO patterns, no diffraction peaks for $CuCl_2$ or Cu_2O can be detected.

Capacities of the electrodes with and without CuO during activation are shown in Fig. 2. It can be noticed that the electrode without additive need eight cycles to be activated and the maximum discharge capacity is 314 mAh g^{-1}. The CuO additive not only reduces the cycle number for activation, but increases the discharge capacity. When 0.5 wt.% CuO is added the activation cycle number is 7 and the maximum discharge capacity is 326 mAh g^{-1}. When 1.0 wt.% or more CuO is added the activation number is 4 or 5, and the maximum discharge capacity is more than 335 mAh g^{-1}, when 3.0 wt.% CuO is added the discharge capacity increases to 341 mAh g^{-1}.

Fig. 3 shows SEM image and EDX analysis of the electrode with 2.0 wt.% CuO addition after 100 cycles. It can be seen some fine spherical particles appear at surface of the alloy particles. Micro-area A corresponds to the alloy basis, B to the spherical particles and C to the particles around the alloy particles. The EDX analysis results are also shown in Fig. 3. It is shown that the element composition of micro-area A is close to that of the alloy except for Mn and Mg element. Mn and Mg element cannot be detected by EDX for they easily enter into the electrolyte during charging/discharging. However, in this micro-area, 13.12 wt.% elemental O can be detected, indicating the alloy is seriously oxidized during the 100 cycles. In micro-area B, a spherical particle can be seen and the Cu content is more obvious, up to 34.78 wt.%. The particle can be considered as Cu reduced from CuO. In Micro-area B a little of Mn can also be detected than the alloy basis, which may result from protection from Cu deposition to the alloy dissolution and in this area no elemental O is detected. Many similar particles as in micro-area B can be found in the SEM image, even between particles and in the cracks of the alloy particles. These particles may be helpful to enhance the electric and heat conductivity between alloy particles and is beneficial to protecting the electrodes from fast capacity degradation. Micro-area C is mainly carbonyl nickel added into the electrode as conductor and linker between alloy particles. As for the elemental K, it can be considered as residual electrolyte solution at the alloy surface.

Fig. 4 shows the cyclic voltammogram of CuO. It can be seen that cyclic voltammogram of CuO shows five noticeable current peaks which correspond to redox reactions in alkaline solution. Two anodic current peaks of E_{O1} (−0.36 V) and E_{O2} (−0.02 V) and three cathodic current peaks of E_{R1} (−0.70 V), E_{R2} (−0.95 V) and E_{R3} (−1.19 V) are observed in the figure. The reduction process of cupric oxide in alkaline solution consisted of two steps [15,20], which can

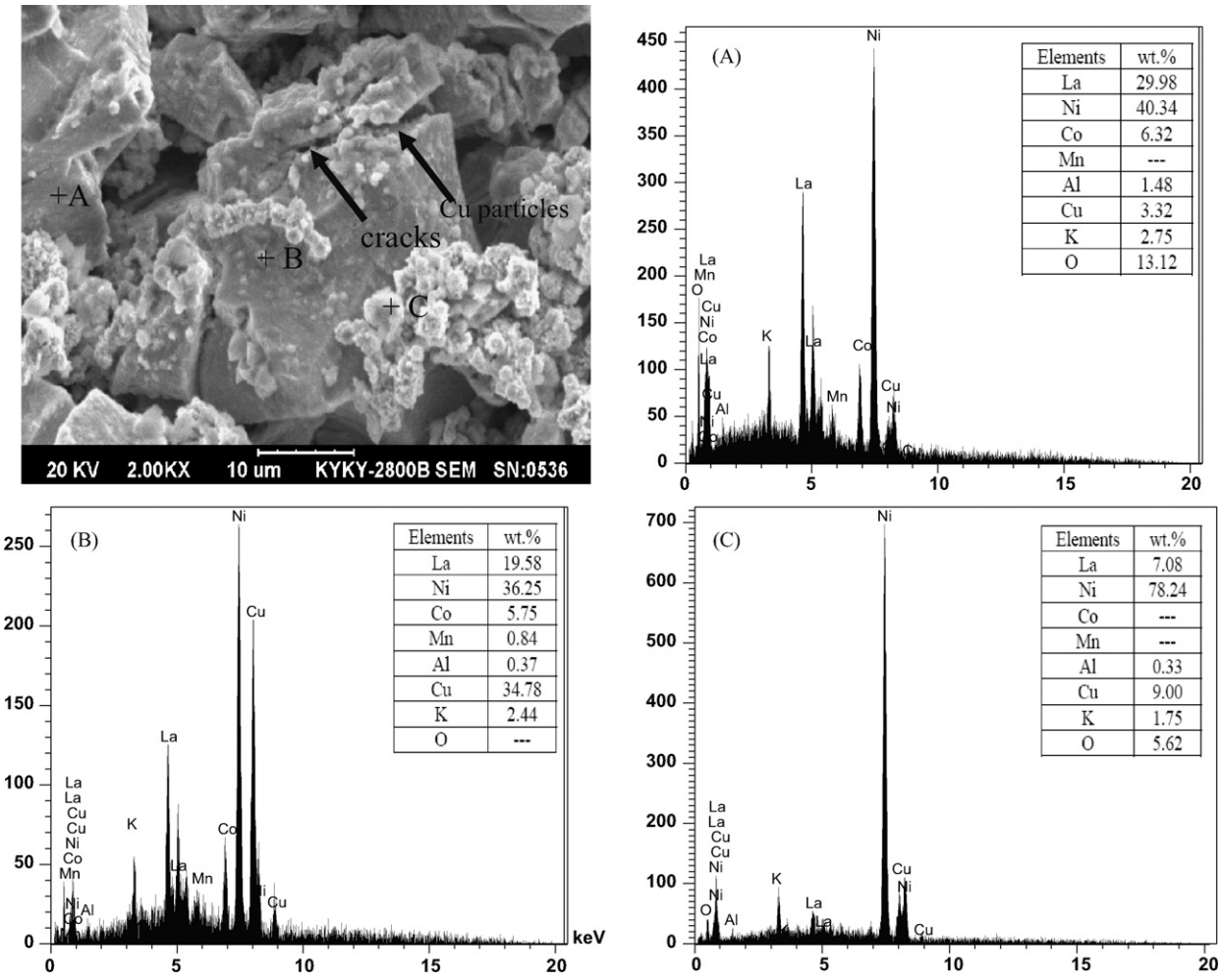

Fig. 3. SEM image and EDX analysis of electrodes with 2.0 wt.% CuO addition.

be described by the following reactions.

$$2CuO + H_2O + 2e^- \rightarrow Cu_2O + 2OH^- \quad (1)$$

$$Cu_2O + H_2O + 2e^- \rightarrow 2Cu + 2OH^- \quad (2)$$

Therefore the cathodic current peak of E_{R1} is attributed to the reduction reaction of CuO to Cu_2O Eq. (1) and the cathodic current peak of E_{R2} is attributed to the reduction reaction of Cu_2O to Cu Eq. (2). Correspondingly, the two anodic current peaks are attributed to the oxidation reaction of Cu to Cu_2O (E_{O1}) and Cu_2O to CuO (E_{O2}). In the potential range −1.2 V to −0.6 V, only reduction reaction of CuO can occur, so in the first charging, Cu particles form in the hydride electrode, while the as-deposited Cu particles will not transfer into CuO again. It is well known that Cu has good heat and electronic conductivity, which can reduce polarization of the anodic electrode reaction, and therefore the maximum discharge capacity is increased.

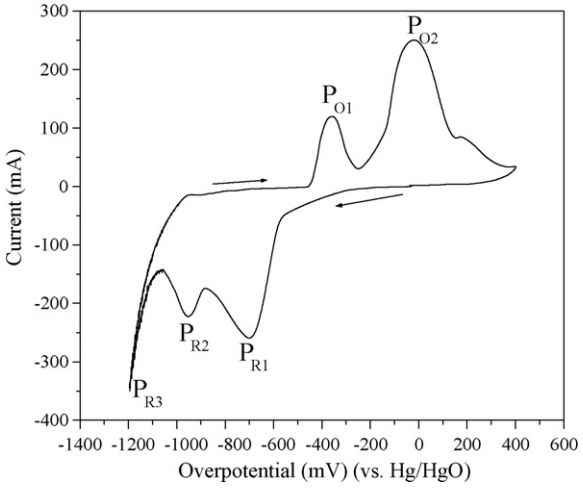

Fig. 4. Cyclic voltammograms of as-prepared CuO.

Fig. 5 shows high rate dischargeability (HRD) of electrodes with and without CuO additives. It is noticed that CuO additives improve the HRD when the discharge current density is larger than 720 mA g^{-1}. At discharge current density of 1440 mA g^{-1}, the HRD is noticeably higher than that of electrode without CuO additives. As the case of CuO additive being 0.5 wt.%, HRD of the electrode reaches up to 59.9%. The increase in high rate dischargeability of CuO-added electrode may be due to good electronic and heat conductivity of as-deposited Cu particles during the charging process.

Fig. 6 shows decrease in discharge capacity of electrodes varying with cycle number. The ratio of discharge capacity at the 40th cycle to maximum discharge capacity (C_{40}/C_{max}) for the CuO-added electrodes is smaller than that of the electrode without CuO addition, indicating faster capacity degradation at the first 40 cycles. However, C_{120}/C_{40} and C_{200}/C_{120} for the CuO-added electrodes is higher than that of the electrode without addition, suggesting that capacity degradation in CuO-added electrodes becomes slower after

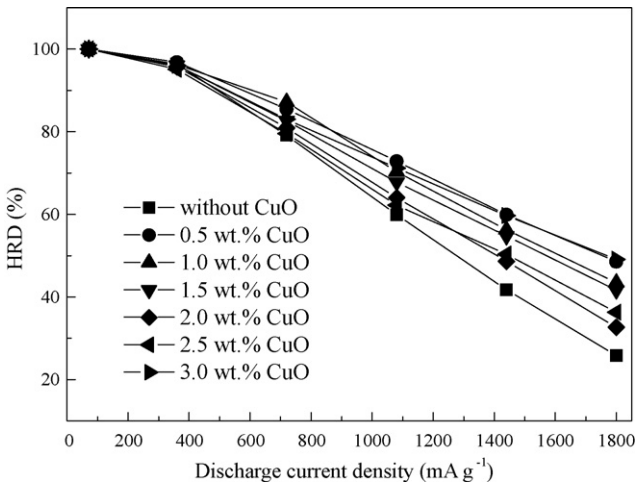

Fig. 5. HRD of electrodes with and without CuO.

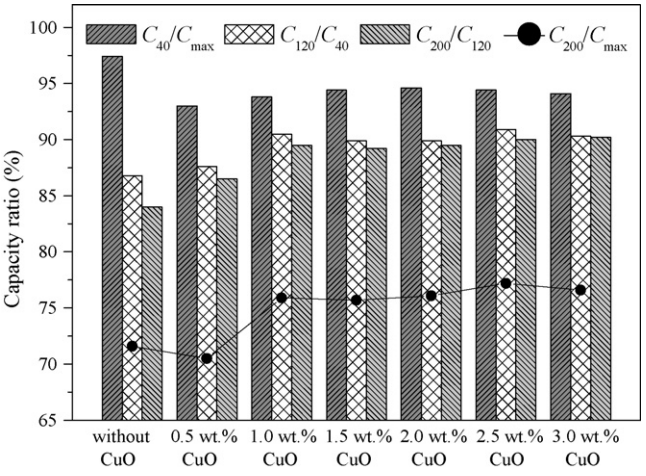

Fig. 6. Cycling stability of electrodes with and without CuO.

40 charge/discharge cycles. This leads directly to improvement in cycling stability, and the discharge capacity retention at the 200th cycle increases from 71.6% (blank electrode) to 77.2% (2.5 wt.% CuO electrode).

As can be seen from SEM and EDX analysis in Fig. 3 CuO transfers to fine Cu particles and Cu particles deposit at surface of the alloy, protecting constituent elements, such as La, Mg and Mn from corrosion by the strong alkaline electrolyte, and thus reduces discharge capacity degradation of the electrodes.

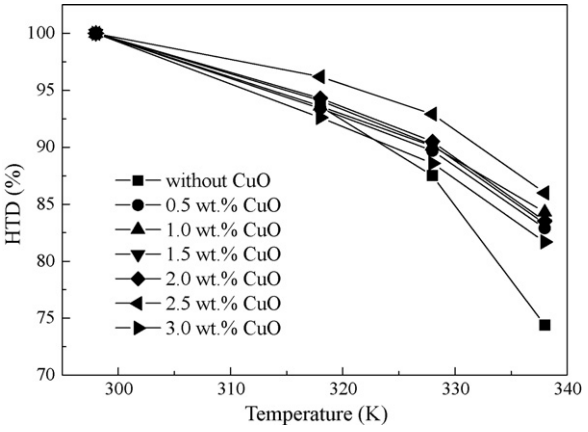

Fig. 7. HTD of electrodes with and without CuO.

Fig. 7 shows high temperature dischargeability (HTD) of the electrodes with and without CuO additives. CuO additives improve HTD of the electrodes, especially with temperature higher than 328 K. The electrode with 2.5 wt.% CuO additive has much better HTD than the others and its HTD at 333 K reaches 86.0%, 11.6% higher than that of the blank electrode (74.4%).

4. Conclusions

The $La_{0.88}Mg_{0.12}Ni_{2.95}Mn_{0.10}Co_{0.55}Al_{0.10}$ alloy consists of $CaCu_5$-type $LaNi_5$ phase, $PuNi_3$-type $LaNi_3$ phase and some minor LaNi impurity. CuO was added to the AB_3-type alloy electrodes in order to improve the electrochemical properties. SEM and cyclic voltammogram show that CuO can be reduced to fine Cu particles during charge processing, depositing at surface of alloy particles. The maximum discharge capacity increases from 314 mAh g^{-1} (blank electrode) to 341 mAh g^{-1} (3.0 wt.% CuO). The high rate dischargeability increases after CuO is added, and the electrode with 0.5 wt.% CuO addition exhibits HRD of 59.9% at 1440 mA g^{-1}. The cycling stability is greatly improved by CuO addition. When the charge/discharge cycle number is more than 40, capacity of electrodes with 1.0 wt.% or more CuO addition decreases more slowly that of the blank one. And the discharge capacity retention rate at the 200th cycle increases from 71.6% (blank electrode) to 77.2% (2.5 wt.% CuO electrode). CuO additive also improves high temperature dischargeability of the electrodes.

Acknowledgements

This work was financially supported by the National Natural Science Foundation of China (20673093), the Natural Science Foundation of Hebei Province (B2007000303) and Support Program for Hundred Excellent Innovation Talents from the Universities and Colleges of Hebei Province.

References

[1] F.C. Ruiz, E.B. Castro, S.G. Real, H.A. Peretti, A. Visintin, W.E. Triaca, Int. J. Hydrogen Energy 33 (13) (2008) 3576–3580.
[2] M. Ben Moussa, M. Abdellaoui, H. Mathlouthi, J. Lamloumi, A. Percheron Guégan, J. Alloys Compd. 458 (2008) 410–414.
[3] S. Bliznakov, E. Lefterova, N. Dimitrov, K. Petrov, A. Popov, J. Power Sources 176 (2008) 381–386.
[4] T. Kohno, H. Yoshida, F. Kawashima, T. Inaba, I. Sakai, M. Yamamoto, M. Kanda, J. Alloys Compd. 311 (2000) L5–L7.
[5] F. Li, K. Young, T. Ouchi, M.A. Fetcenko, J. Alloys Compd. 471 (2009) 371–377.
[6] Y. Li, S.M. Han, J.H. Li, X.L. Zhu, L. Hu, Mater. Chem. Phys. 108 (2008) 92–96.
[7] R.V. Denys, B. Riabov, V.A. Yartys, R.G. Delaplane, M. Sato, J. Alloys Compd. 446-447 (2007) 166–172.
[8] Y.J. Chai, K. Sakaki, K. Asano, H. Enoki, E. Akiba, T. Kohno, Scripta Mater. 57 (2007) 545–548.
[9] J.B. Wu, J.P. Tu, Z. Yu, X.B. Zhang, J. Electrochem. Soc. 153 (10) (2006) A1847–A1851.
[10] H.Y. Zhang, Y.T. Chen, Q.F. Zhu, G.Q. Zhang, Y.M. Chen, Int. J. Hydrogen Energy 33 (2008) 6704–6709.
[11] X.Z. Zhang, Z.X. Gong, S.M. Zhao, M.M. Geng, Y. Wang, D.O. Northwood, J. Power Sources 175 (2008) 630–634.
[12] G. Barkhordarian, T. Klassen, R. Bormann, Scripta Mater. 49 (2003) 213–217.
[13] Z.G. Huang, Z.P. Guo, A. Calka, D. Wexler, C. Lukey, H.K. Liu, J. Alloys Compd. 422 (2006) 299–304.
[14] P. Zhang, X.D. Wei, Y.N. Liu, J.W. Zhu, G. Yu, Int. J. Hydrogen Energy 33 (2008) 1304–1309.
[15] S. Zhang, P. Shi, C. Deng, Solid State Ionics 177 (2006) 1193–1197.
[16] G. Dong, J. Du, L. Zhu, B. Wu, J. Chin. Rare Earth Soc. 24 (4) (2006) 465–469.
[17] C. Wang, M. Marrero-Cruz, M.P. Soriaga, D. Serafini, S. Srinivasan, Electrochim. Acta 47 (2002) 1069–1078.
[18] N. Hanada, T. Ichikawa, S. Hino, H. Fujii, J. Alloys Compd. 420 (2006) 46–49.
[19] T. Tanaka, M. Kuzuhara, M. Watada, M. Oshitani, J. Alloys Compd. 408–412 (2006) 323–326.
[20] H.H. Strehblow, V. Maurice, P. Marcus, Electrochim. Acta 46 (2001) 3755–3766.